

# RSC Advances



This is an *Accepted Manuscript*, which has been through the Royal Society of Chemistry peer review process and has been accepted for publication.

*Accepted Manuscripts* are published online shortly after acceptance, before technical editing, formatting and proof reading. Using this free service, authors can make their results available to the community, in citable form, before we publish the edited article. This *Accepted Manuscript* will be replaced by the edited, formatted and paginated article as soon as this is available.

You can find more information about *Accepted Manuscripts* in the [Information for Authors](#).

Please note that technical editing may introduce minor changes to the text and/or graphics, which may alter content. The journal's standard [Terms & Conditions](#) and the [Ethical guidelines](#) still apply. In no event shall the Royal Society of Chemistry be held responsible for any errors or omissions in this *Accepted Manuscript* or any consequences arising from the use of any information it contains.



PCCP

ARTICLE

## Intrinsic $[\text{VO}_4]^{3-}$ emission of cesium vanadate $\text{Cs}_5\text{V}_3\text{O}_{10}$

Yinfu Pu,<sup>a</sup> Yanlin Huang,<sup>a</sup> Taiju Tsuboi,<sup>b</sup> Han Cheng<sup>c</sup> and Hyo Jin Seo\*<sup>c</sup>

Received 00th January 20xx,  
Accepted 00th January 20xx

DOI: 10.1039/x0xx00000x

www.rsc.org/

Polycrystalline  $\text{Cs}_5\text{V}_3\text{O}_{10}$  micro-particles were synthesized by the solid-state reaction. The vanadate shows intrinsic self-activated luminescence of a single broad band with a peak at 520 nm, extending from about 400 nm to 720 nm. This asymmetric band is decomposed to two bands due to the electronic transitions from the  ${}^3\text{T}_1$  and  ${}^3\text{T}_2$  excited states to  ${}^1\text{A}_1$  ground state in  $[\text{VO}_4]^{3-}$  centers. Same emission band was obtained from micro- and nano-particles. It is suggested that the broadening of the emission band arises from single  $[\text{VO}_4]^{3-}$  molecule. The emission and decay curve profiles indicate that the emission is due to not different kinds of  $[\text{VO}_4]^{3-}$  centers but only one kind of  $[\text{VO}_4]^{3-}$  center. When temperature is increased from 10 K to 450 K, the emission intensity increases below 150 K and decreases above 150 K, and unusual blue shift is observed. The observed temperature dependence is understood by relaxation processes of the emitting  ${}^3\text{T}_1$  and  ${}^3\text{T}_2$  states including the thermal feeding by the lower-energy  ${}^3\text{T}_1$  state to the higher-energy  ${}^3\text{T}_2$  state.

### 1. Introduction

Luminescent materials have been widely employed for optoelectronic technologies, e.g., for photonic/electronic integration, solid-state lighting, and labels in biological research, etc.<sup>1-4</sup> Of various luminescent materials, vanadates have been also used for solid state lighting, display, and pigments.<sup>5-6</sup> Vanadates are compounds which contain vanadium V ion surrounded by oxygen O ions. Many kinds of vanadate materials have been synthesized. The samples are  $\text{YVO}_4$ ,  $\text{AVO}_3$  (A: Li, Na, K, Rb, Cs),  $\text{M}_2\text{V}_2\text{O}_7$  (M: Mg, Ca, Sr, Ba, Zn),  $\text{M}_3\text{V}_2\text{O}_8$  (M: Mg, Ca, Sr, Ba, Zn),  $\text{Zn}_3(\text{VO}_4)_2$ ,  $\text{CsK}_2\text{Gd}[\text{VO}_4]_2$ , and  $\text{Ca}_2\text{NaMg}_2\text{V}_3\text{O}_{12}$ . Recently a lot of studies have been made on vanadates doped with lanthanide ions. The lanthanide-doped vanadate nanoparticles exhibit efficient emission from lanthanides by energy transfer from vanadate host, and wide colour tuning is easily made by selection of elements of lanthanide, which can be applied in many fields, such as cathode ray tubes, lamps, X-ray detectors, biosensors, and solid-state laser.<sup>7-13</sup> In these nanoparticles, emission from vanadate host is not observed or considerably weak because of highly efficient energy transfer from host to the activator. It has been observed that non-doped vanadates show a broad emission band in visible spectral region as mentioned later. We are interesting in the luminescence of vanadate itself, i.e., intrinsic and self-activated luminescence from non-doped vanadates.

The origin of the intrinsic luminescence from vanadates has

been assigned to the charge transfer (CT) transitions from the HOMO (highest occupied molecular orbital) level, which is composed of O 2p nonbonding orbitals, to the LUMO (lowest unoccupied molecular orbital) level, which is composed of antibonding V 3d orbitals and O 2p orbitals, in tetrahedral  $[\text{VO}_4]^{3-}$ .<sup>14-16</sup> These molecular orbitals form the ground  ${}^1\text{A}_1$  state and the excited  ${}^1\text{T}_1$ ,  ${}^1\text{T}_2$ ,  ${}^3\text{T}_1$ , and  ${}^3\text{T}_2$  states.<sup>17,18</sup> The electronic transitions of  ${}^1\text{A}_1 \rightarrow ({}^1\text{T}_1, {}^1\text{T}_2)$  give rise to a doublet-structured broad and intense CT absorption band in the UV region in all the vanadates, while a broad and intense CT emission band is observed at 400-720 nm region, which is due to the transitions of  $({}^3\text{T}_1, {}^3\text{T}_2) \rightarrow {}^1\text{A}_1$ .<sup>19-22</sup> This luminescence mechanism is based on the electronic transitions in  $[\text{VO}_4]^{3-}$ , which is called  $[\text{VO}_4]^{3-}$  model hereafter.

The broadband emission and UV absorption properties make vanadates suitable for solar cell, because the visible photoluminescence (PL) which is generated under excitation with UV light from the sun is absorbed by the current silicon solar cell materials. Of many kinds of vanadates, some vanadates show high PL quantum efficiency (PQE). For example,  $\text{RbVO}_3$  and  $\text{CsVO}_3$  show PQE of 79 % and 87 %, respectively, compared to PQE=4 % of  $\text{KVO}_3$ .<sup>16</sup> Similarly,  $\text{Zn}_3\text{V}_2\text{O}_8$  shows high PQE value, 52 %, compared to 6 % of  $\text{Mg}_3\text{V}_2\text{O}_8$ , although the two  $\text{M}_3\text{V}_2\text{O}_8$  (A: Mg and Zn) materials show the same broad emission band extending from 410 nm to 900 nm.<sup>16</sup>

Recently, we reported that lanthanide-free  $\text{Cs}_5\text{V}_3\text{O}_{10}$  shows the  $[\text{VO}_4]^{3-}$  emission with a high PQE of 85.2 % under UV light. This vanadate also gives intense scintillating emission under X-ray excitation.<sup>23</sup> Therefore  $\text{Cs}_5\text{V}_3\text{O}_{10}$  is expected to be useful for lighting, display, and scintillation. However, the photo-physical nature has not been clarified. For example, (1) the reason why broad emission band is observed for  $\text{Cs}_5\text{V}_3\text{O}_{10}$  is unknown, (2) it is unknown whether the width and peak wavelength of the emission band change by particle size, (3) it is unknown whether only one or different kinds of luminescent  $[\text{VO}_4]^{3-}$  centers are present in

<sup>a</sup> College of Chemistry, Chemical Engineering and Materials Science, Soochow University, Suzhou 215123, China.

<sup>b</sup> Kyoto Sangyo University, Kamigamo, Kita-ku, Kyoto 603-8555, Japan.

<sup>c</sup> Department of Physics and Interdisciplinary Program of Biomedical, Mechanical & Electrical Engineering, Pukyong National University, Busan 608-737, Republic of Korea.

E-mail: [hjseo@pknu.ac.kr](mailto:hjseo@pknu.ac.kr) (Hyo Jin Seo) Tel.: +82-51-629 5568; fax: +82-51-6295549.

Cs<sub>5</sub>V<sub>3</sub>O<sub>10</sub> sample, and (4) the relaxation process in the excited states of [VO<sub>4</sub>]<sup>3-</sup> is still unknown. The present work was undertaken to try to clarify these points.

It is suggested that an unusual broadband emission observed from CdSe is caused by ultra-small CdSe nanocrystals.<sup>24</sup> In our previous paper, we synthesized Cs<sub>5</sub>V<sub>3</sub>O<sub>10</sub> nano-particles with diameter size of 47-135 nm by the Pechini method.<sup>23</sup> In the present work, we make Cs<sub>5</sub>V<sub>3</sub>O<sub>10</sub> micro-crystals by the solid state reaction, to clarify whether the size of Cs<sub>5</sub>V<sub>3</sub>O<sub>10</sub> particles is responsible for the broadening of the emission band or not. Besides these purposes of the present work, there is another purpose. Recently Wang et al observed a broad emission band with a peak at 546.4 nm, which extends from 420 to 700 nm, from Zn<sub>3</sub>(VO<sub>4</sub>)<sub>2</sub> vanadate microspheres.<sup>25</sup> Although the [VO<sub>4</sub>]<sup>3-</sup> model has been used in many papers,<sup>14-22</sup> they have suggested that the 546.4 nm vanadate emission might be ascribed to zinc vacancies existed in Zn<sub>3</sub>(VO<sub>4</sub>)<sub>2</sub>. Here we investigate whether the vacancy model is acceptable to the emission of Cs<sub>5</sub>V<sub>3</sub>O<sub>10</sub>.

## 2. Experimental

The preparations of Cs<sub>5</sub>V<sub>3</sub>O<sub>10</sub> powders were carried out by solid state reactions. The starting chemicals were high-purity Cs<sub>2</sub>CO<sub>3</sub> and V<sub>2</sub>O<sub>5</sub>. The stoichiometric materials were thoroughly mixed together. Firstly, the mixtures were heated at 350 °C for 6 h. Then the powders were thoroughly ground to a homogeneous mixture; secondly, the mixture was sintered at 680 °C for 6 h.

The photoluminescence (PL) and PL excitation (PLE) spectra at room temperature were recorded by a Perkin-Elmer LS-50B luminescence spectrometer and a Hitachi F-4500 fluorescence spectrophotometer. The PL and PLE spectra at various temperatures between 10 K and 450 K were measured with a Spex Fluorolog-3 spectrophotometer under a 500 W Xe-lamp excitation. The PL lifetime measurements were made using the third harmonics (355 nm) of a Spectron Laser Sys. SL802G pulsed Nd:YAG (yttrium aluminum garnet) laser with a pulse energy of 5 mJ, repetition rate of 10 Hz, and duration of 5 ns at 10-300 K (gas helium flow). The luminescence was dispersed by a 75 cm monochromator (Acton Research Corp. Pro-750) and observed with a photomultiplier tube (Hamamatsu R928). The decays were recorded by the 500 MHz digital oscilloscope (Tektronix DPO3054). A filter was used to avoid the intense singles from the laser scattering.

## 3. Results and discussion

The X-ray diffraction (XRD) pattern of the synthesized Cs<sub>5</sub>V<sub>3</sub>O<sub>10</sub> was examined to characterize the phase purity and crystallinity. Fig. 1 shows the XRD pattern. It is found that all the diffraction peaks are in good agreement with the standard card PDF2# 50-0027 in the International Center for Diffraction Data (ICDD) database. No impurity lines are observed. The results indicate the sample has a pure crystal formation of Cs<sub>5</sub>V<sub>3</sub>O<sub>10</sub>. From the XRD, it is confirmed that the tetrahedral [VO<sub>4</sub>]<sup>3-</sup> ions are formed.

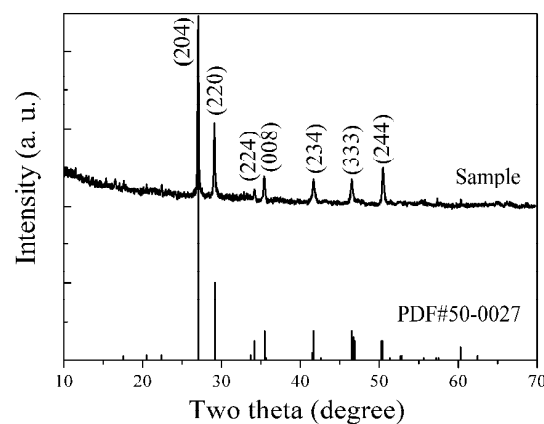


Fig. 1 The typical XRD patterns of Cs<sub>5</sub>V<sub>3</sub>O<sub>10</sub> phosphor and standard PDF2 card No. 50-0027.

The typical scanning electron microscope (SEM) micrograph of Cs<sub>5</sub>V<sub>3</sub>O<sub>10</sub> prepared by the solid-state reaction is shown in Fig. 2. According to the image, the sizes of the synthesized particles are mainly 2-5 μm. Particles with size less than 1 μm are very few, indicating success of micro-particle synthesis. Unlike the round-shape nanoparticles synthesized by the Pechini method,<sup>23</sup> the particles have rectangle-like shape with smooth surface.

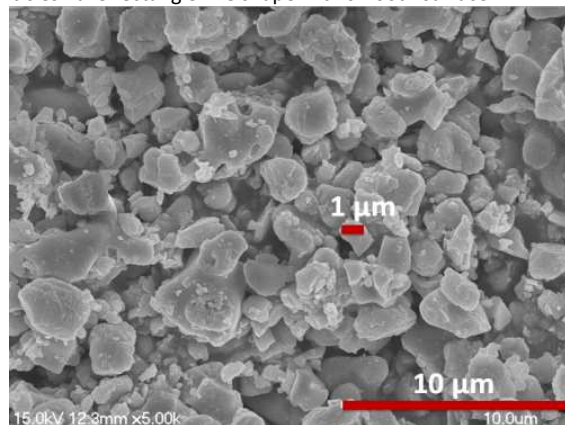
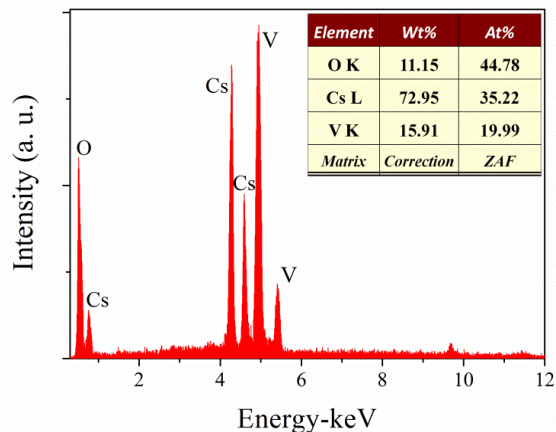


Fig. 2 The typical SEM micrograph of Cs<sub>5</sub>V<sub>3</sub>O<sub>10</sub> particles

The elemental composition was checked by the energy-dispersive X-ray spectroscopy (EDS). Fig. 3 is the EDS spectrum of the synthesized Cs<sub>5</sub>V<sub>3</sub>O<sub>10</sub>. It is confirmed that the synthesized sample has elements of Cs, O, and V. The average Cs/V ratio was measured to be about 1.76. This value is close to the theoretical value (5/3 = 1.67) in stoichiometric chemical formula of Cs<sub>5</sub>V<sub>3</sub>O<sub>10</sub>. These EDS and XRD results indicate our success of synthesis of Cs<sub>5</sub>V<sub>3</sub>O<sub>10</sub> which does not contain any impurity.

We compare the PL spectrum of micro-particles synthesized by the present work with the PL spectrum of nano-particles which was presented in our previous paper,<sup>23</sup> to investigate whether the size of Cs<sub>5</sub>V<sub>3</sub>O<sub>10</sub> particle is responsible for the broadening of emission band. Fig. 4 shows the PL spectra of micro- and nano-particles. Same broad emission band with a peak at 520 nm which extends from 400 nm to 750 nm is obtained from the micro- and nano-particles. Surface effect was expected to appear more strongly for nano-

particles than for micro-particles. However, such an effect was not found. This indicates that the particle size is not responsible for the broadening of the emission band due to  $[\text{VO}_4]^{3-}$ . Observation of the emission due to  $[\text{VO}_4]^{3-}$  confirms non-presence of unintended impurities in our samples, because it has been reported that impurities randomly located in the crystal lattice induce quenching of luminescence of  $\text{YVO}_4$  vanadate at room temperature.<sup>13</sup>



**Fig. 3** EDS spectrum of  $\text{Cs}_5\text{V}_3\text{O}_{10}$ , with indication of the elements.

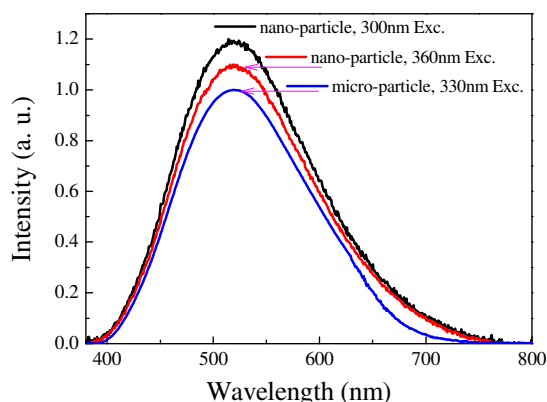


**Fig. 4** PL spectra of micro-particles (red line) excited at 330 nm and nano-particles excited at 300 nm (blue) and 360 nm (black).

The emission from single molecules, which are dispersed in solution, is broad by the charge transfer and electron-phonon interaction within the single molecule.<sup>26</sup> **Therefore** it is suggested that the broad emission of vanadates arises from single  $[\text{VO}_4]^{3-}$  molecules which are distributed uniformly in micro- and nano-particles without any electronic interaction with neighboring  $\text{VO}_4^{3-}$  molecule and with defects. As a result, the  $\text{Cs}_5\text{V}_3\text{O}_{10}$  nano- and micro-particles have shown the same emission band.

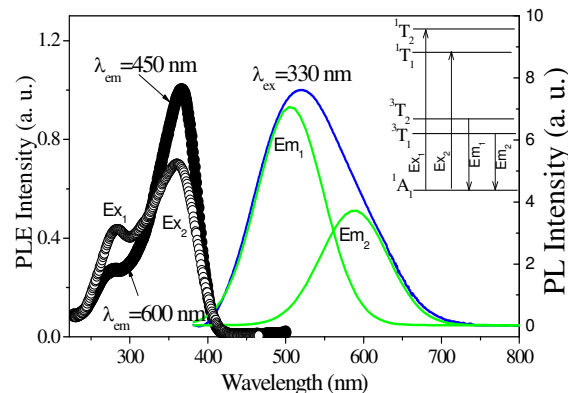


**Fig. 5** Photoluminescence (PL) and PL excitation (PLE) spectra of  $\text{Cs}_5\text{V}_3\text{O}_{10}$  at 300 K. Inset shows a diagram showing the processes of excitation and emission.

The 520 nm emission band is asymmetric. This band is decomposed to two sub-bands (called  $\text{Em}_1$  and  $\text{Em}_2$  at high- and low-energy sides, respectively) as shown in **Fig. 5**. Similar decomposition has been made in various vanadates.<sup>16,20,22</sup> The  $\text{Em}_1$  and  $\text{Em}_2$  sub-bands with peaks at about 507 and 588 nm are attributed to the transitions from the  $^3\text{T}_2$  and  $^3\text{T}_1$  states to the ground state  $^1\text{A}_1$ , respectively as indicated inset **Fig. 5**. And **Fig. 5** also presents the PLE spectrum for the 450 nm  $\text{Em}_1$  emission and the PLE spectrum for the 600 nm  $\text{Em}_2$  emission of  $\text{Cs}_5\text{V}_3\text{O}_{10}$  micro-particles. Each of the two PLE spectra consists of two bands with the same peaks at 280 and 365 nm. The 280 and 365 nm PLE bands are called  $\text{Ex}_1$  and  $\text{Ex}_2$ , respectively. These two absorption bands in the PLE spectra correspond to the transition from the ground state  $^1\text{A}_1$  to the  $^1\text{T}_2$  and  $^1\text{T}_1$  states, respectively, as indicated in inset of **Fig. 5**. The  $\text{Ex}_1$  and  $\text{Ex}_2$  absorption bands are observed in  $\text{Cs}_5\text{V}_3\text{O}_{10}$  nano-particles too.<sup>23</sup> The double peak of  $\text{Ex}_1$  and  $\text{Ex}_2$  in the PLE spectrum has been also observed in various vanadates such as  $\text{M}_2\text{V}_2\text{O}_7$  (M: Mg, Ca, Sr, Ba, and Zn),<sup>20</sup>  $\text{AVO}_3$  (A: K, Rb, Cs) and  $\text{M}_3\text{V}_2\text{O}_8$  (M: Mg, Zn),<sup>16</sup> and  $\text{GdVO}_4$ .<sup>27</sup> This confirms that the  $\text{Ex}_1$  and  $\text{Ex}_2$  bands arise from  $[\text{VO}_4]^{3-}$  ion which is common component of vanadate materials.

It has been observed in  $\text{Cs}_5\text{V}_3\text{O}_{10}$  nanoparticles that the excitations into the  $\text{Ex}_1$  and  $\text{Ex}_2$  bands gives the same emission band<sup>23</sup> as shown in **Fig. 4** by blue and black curves, respectively. The same was also observed for  $\text{Cs}_5\text{V}_3\text{O}_{10}$  micro-particles. It is noted that the PLE spectrum for the  $\text{Em}_1$  emission give different intensity ratio of the  $\text{Ex}_1$  and  $\text{Ex}_2$  bands from the PLE spectrum for the  $\text{Em}_2$  emission although the same  $\text{Ex}_1$  and  $\text{Ex}_2$  peak wavelengths are observed for the two PLE spectra (**Fig. 5**). From this result, it might be suggested that different luminescent  $[\text{VO}_4]^{3-}$  centers are present in  $\text{Cs}_5\text{V}_3\text{O}_{10}$  micro-particles. If so, it is difficult to explain the reasons (1) why same  $\text{Ex}_1$  and  $\text{Ex}_2$  peak wavelengths are observed for the two PLE spectra and (2) why the same emission band is observed by the  $\text{Ex}_1$  and  $\text{Ex}_2$  excitations. The reason for the different intensity ratio of the  $\text{Ex}_1$  and  $\text{Ex}_2$  bands would be suggested as follows, based on only one kind of luminescent center. The probability of non-radiative transition from the excited  $^1\text{T}_2$  and  $^1\text{T}_1$  states to the  $^3\text{T}_2$  state, which leads to the  $\text{Em}_1$  emission, is different from the

probability of non-radiative transition from the excited  $^1T_2$  and  $^1T_1$  states to the  $^3T_1$  state, which leads to the  $Em_2$  emission. As the result, the different intensity ratio of the  $Ex_1$  and  $Ex_2$  bands was observed.

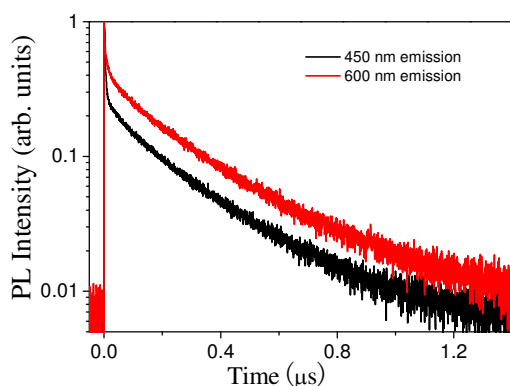


Fig. 6 PL decay curves of 600 and 450 nm emissions at 10 K.

The idea of presence of only one kind of luminescent center is supported by the PL lifetime measurements. Fig. 6 shows the PL decay curves of 450 and 600 nm emissions. The 450 and 600 nm emissions are selected as emission of the  $Em_1$  and  $Em_2$  emissions, respectively. A fast drop is observed at about 0-0.008  $\mu$ s (i.e., 0-8 ns) in each of two emission decay curves. This drop is due to our pulsed laser which was used as excitation, because the laser has duration of 5 ns. The two decay curves are quite similar to each other. This indicates that (1) the  $Em_1$  and  $Em_2$  emissions occur after fast thermal equilibrium between the  $^3T_2$  and  $^3T_1$  excited states, and (2) the emission arises from not different kinds of  $[VO_4]^{3-}$  luminescent center but only one kind of  $[VO_4]^{3-}$  luminescent center. If different kinds of luminescence centers are present, it is expected that the  $Em_1$  and  $Em_2$  emissions give quite different PL lifetimes.

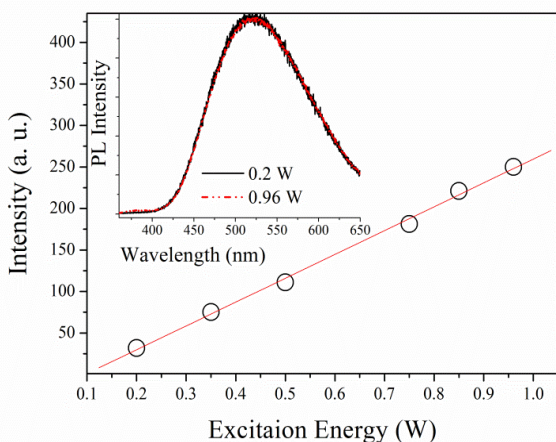


Fig. 7 The dependence of emission intensity of  $Cs_5V_3O_{10}$  on excitation intensity; Inset is the comparison of emission spectra between the power of 0.2 W and 0.96 W.

As mentioned above, we have suggested that the broad emission of vanadates arises from  $[VO_4]^{3-}$  molecules which do not have electronic interaction with defects. To check the non-interaction with defects, we investigate the dependence of emission intensity on the excitation intensity. It is known that the PL intensity shows saturation at high excitation intensities if the emission arises from permanent defects as these traps.<sup>28,29</sup> Fig. 7 shows the  $[VO_4]^{3-}$  emission intensity plotted against the excitation intensity. It is observed that the emission intensity increases linearly with increasing the excitation power from 0.2 to 0.92 W. No PL saturation is observed. These results indicate that the defect is not responsible for the emission.

If defects such as photo-generated trap are generated at high excitation intensities, the emission band shape is changed with increasing the excitation intensity.<sup>30,31</sup> No change was observed in band-shape of emission from  $Cs_5V_3O_{10}$  with increasing excitation intensity. For example, the same emission line shape is obtained at low and high excitation powers of 0.2 W and 0.96 W, respectively (inset of Fig. 7). This indicates that emissive defects such as photo-generated trap are not generated in  $Cs_5V_3O_{10}$  at high excitation intensities.

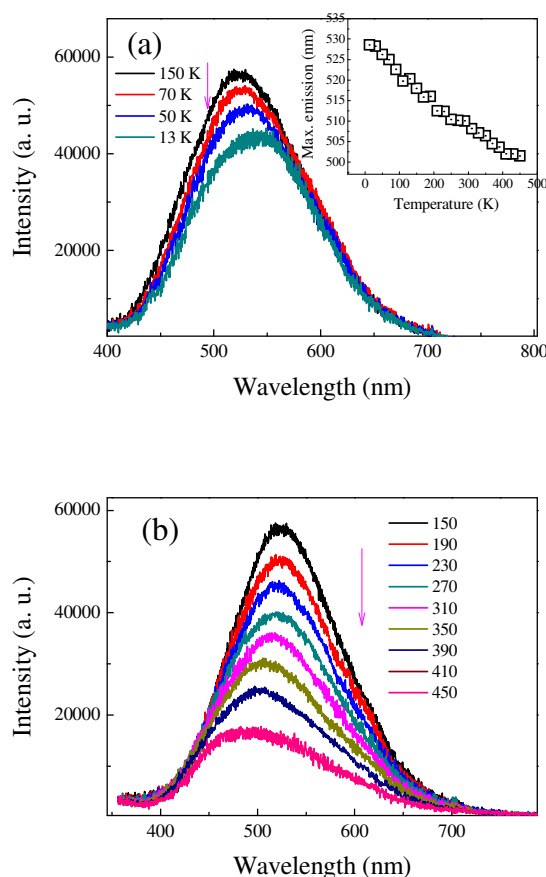


Fig. 8 Temperature dependences of the emission spectra of  $Cs_5V_3O_{10}$  (a, b) and the peak wavelength (inset of (a)).

Fig. 8 shows the temperature dependence of the emission spectra of Cs<sub>5</sub>V<sub>3</sub>O<sub>10</sub> and the peak wavelength of the emission band. The emission intensity is plotted against temperature in Fig. 9. Two unusual results are found regarding the emission intensity and emission peak shift.

Firstly, the emission intensity increases from 10 K to 150 K, while decreases quickly above 150 K (Fig. 9). The thermal quenching has been described by Eq. (1), on the model by Struck and Fonger.<sup>32-35</sup> This equation was obtained for the luminescence center where the electrons in the emitting state are relaxed to the ground state by (1) the radiative transition process and (2) the non-radiative transition process through thermal activation with activation energy  $\Delta E$ .

$$I_T = I_0 / [1 + c \text{Exp}(-\Delta E / kT)] \quad (1)$$

Here  $I_T$  is the intensity at temperature  $T$ ,  $I_0$  is intensity at near 0 K,  $c$  is a rate constant for thermally activated escape. In case of the emission from Cs<sub>5</sub>V<sub>3</sub>O<sub>10</sub>,  $\Delta E$  is attributed to the energy from the upper emitting state <sup>3</sup>T<sub>2</sub> to the crossing point of the <sup>3</sup>T<sub>2</sub> state and the <sup>1</sup>A<sub>1</sub> ground state in the configuration coordinate diagram. The electrons which are thermally excited to the crossing point are relaxed to the <sup>1</sup>A<sub>1</sub> ground state non-radiatively.

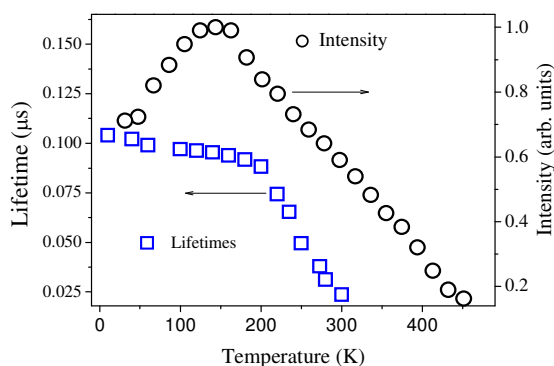


Fig. 9 the temperature dependences of the integrated emission intensity (a, right scale) and the average lifetimes (b, left scale). The intensities were normalized at the maximum of the emission intensity at 145 K.

Eq. (1) indicates that the emission intensity is nearly constant at low temperatures with increasing temperature from 0 K until a certain temperature (called quenching temperature,  $T_q$ ) and suddenly decreases nearly exponentially at high temperatures above  $T_q$ . The luminescence of Cs<sub>5</sub>V<sub>3</sub>O<sub>10</sub>, however, doesn't obey Eq. (1) especially at low temperatures (10-150 K). The intensity increases at lower temperature than the quenching temperature of 150 K as shown in Fig. 9. By taking into account thermal feeding by the <sup>3</sup>T<sub>1</sub> state to the upper <sup>3</sup>T<sub>2</sub> state,<sup>18</sup> we suggest that this unusual increase of the emission intensity at low temperatures is understood as follows.

At low temperatures below 150 K where the thermal activation to the crossing point is not effective, the <sup>3</sup>T<sub>2</sub> state is thermally fed by the lower-energy <sup>3</sup>T<sub>1</sub> state with increasing temperature from 10 K. The transition probability between the <sup>1</sup>T<sub>2</sub> state and <sup>1</sup>A<sub>1</sub> state is

higher than the probability between the <sup>1</sup>T<sub>1</sub> state and <sup>1</sup>A<sub>1</sub> state.<sup>18</sup> It is suggested that same is true for the case of the transition probabilities from the <sup>3</sup>T<sub>2</sub> and <sup>3</sup>T<sub>1</sub> state, i.e., the transition probability between the <sup>3</sup>T<sub>2</sub> state and <sup>1</sup>A<sub>1</sub> state is higher than the probability between the <sup>3</sup>T<sub>1</sub> state and <sup>1</sup>A<sub>1</sub> state. In fact, it is observed that the emission Em<sub>1</sub> from the <sup>3</sup>T<sub>2</sub> state is higher than the intensity Em<sub>2</sub> from the lower-energy <sup>3</sup>T<sub>1</sub> state (Fig. 5). Therefore, the increase of the total luminescence below 150 K is due to the increase of population of the <sup>3</sup>T<sub>2</sub> state, which is enhanced with increasing temperature.

Secondly, unlike most luminescent centers, the emission of Cs<sub>5</sub>V<sub>3</sub>O<sub>10</sub> shifts to high-energy with increasing temperature (inset of Fig. 8 a). It is suggested that the observed blue-shift is understood as follows. Of the two emitting states <sup>3</sup>T<sub>1</sub> and <sup>3</sup>T<sub>2</sub>, the population of the upper <sup>3</sup>T<sub>2</sub> state increases by the thermal feeding by the lower <sup>3</sup>T<sub>1</sub> state with increasing temperature, leading to enhancement of the rate of the intensity of emission from the higher-energy <sup>3</sup>T<sub>2</sub> state to the intensity of emission from the lower-energy <sup>3</sup>T<sub>1</sub> state. In this way we can understand the observed blue shift. This is consistent with the suggestion<sup>36</sup> that thermally active phonons assist jumping of electrons from a lower-energy excited state to a higher-energy excited state.

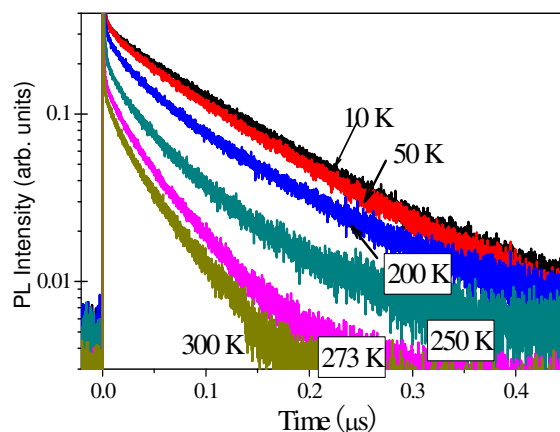


Fig. 10 The decay profiles of Cs<sub>5</sub>V<sub>3</sub>O<sub>10</sub> at 10, 50, 200, 250, 273 and 300 K under excitation with 355 nm laser.

Fig. 10 shows the PL decay profiles of Cs<sub>5</sub>V<sub>3</sub>O<sub>10</sub> at various temperatures. All the decay curves are non-exponential. The decay curve at 10 K extends over 0.7 μs to 1.4 μs (see also Fig. 6), and the decay curve at 300 K extends to 0.2 μs. Such long-time decay profiles indicate that the emission is not fluorescence (which has usually with nano-sec time scale as the emission from LED) but phosphorescence. This supports the idea that the emission of Cs<sub>5</sub>V<sub>3</sub>O<sub>10</sub> is caused by the electronic transitions from the triplet <sup>3</sup>T<sub>1</sub> and <sup>3</sup>T<sub>2</sub> states to the ground state <sup>1</sup>A<sub>1</sub>. These transitions are spin-forbidden. However, intense emission has been observed in various vanadates including Cs<sub>5</sub>V<sub>3</sub>O<sub>10</sub>. The intense emission is caused by the heavy atom effect due to vanadium ion in [VO<sub>4</sub>]<sup>3-</sup>, which leads to the mixing of the singlet <sup>1</sup>T<sub>1</sub> and <sup>1</sup>T<sub>2</sub> states to the triplet <sup>3</sup>T<sub>1</sub> and <sup>3</sup>T<sub>2</sub> states by strong spin-orbit coupling.

If the vacancy gives rise to the vanadate emission as suggested by Wang et al who observed broad band emission from  $\text{Zn}_3(\text{VO}_4)_2$ ,<sup>25</sup> it is difficult to explain why the phosphorescence is observed. It is conceivable that the defects in lattice such as vacancy give rise to quenching of emission.<sup>13</sup> If vacancy gives rise to emission, the peak wavelength and band width of the observed emission band are expected to depend on the metal elements in vanadates largely, as the cases of color centers in alkali halide crystals.<sup>37</sup> However, the emission band profiles observed in various vanadates are almost same. Therefore it is suggested that the  $[\text{VO}_4]^{3-}$  model is more reliable than the vacancy model to understand the observed various optical properties such as phosphorescence, strong emission intensity, and the doublet structure of the PL and PLE bands.

The non-exponential decay curves can be fitted to the average lifetime expressed by Eq. (2).<sup>38</sup>

$$\tau_{\text{average}} = \frac{\int_0^{\infty} I(t) dt}{\int_0^{\infty} I(t) dt} \quad (2)$$

where  $I(t)$  is the emission intensity at time  $t$  after the excitation. From 200 K to 300 K, the average lifetime becomes short from 0.089 to 0.0245  $\mu\text{s}$ .

The emission lifetime is plotted against temperature in Fig. 9. It is observed that the PL lifetime becomes short gradually in the range of 10–200 K, while it becomes short quickly from about 200 K with increasing temperature. The shortening of lifetime at high temperatures is understood as follows.

The parabola potential of the emitting states  ${}^3\text{T}_1$  and  ${}^3\text{T}_2$  has crossing points with the potential of the  ${}^1\text{A}_1$  ground state in the configuration coordinate diagram. The electrons which are thermally excited to the crossing points from the  ${}^3\text{T}_1$  and  ${}^3\text{T}_2$  states are relaxed to the  ${}^1\text{A}_1$  ground state non-radiatively at high temperatures. That is, the  ${}^3\text{T}_1$  and  ${}^3\text{T}_2$  states have two relaxation processes to the  ${}^1\text{A}_1$  state: one is radiative direct transitions and the other is non-radiative transition through the crossing points. The coexistence of these two processes leads to the shortening of the lifetime with increasing temperature because the thermal activation rate is enhanced with increasing temperature. This explanation is based on the  $[\text{VO}_4]^{3-}$  model, not on the defect model. Therefore, it is confirmed from the temperature dependence of the PL lifetime that the  $[\text{VO}_4]^{3-}$  model is more reliable than the defect model.

## 4 Conclusions

$\text{Cs}_5\text{V}_3\text{O}_{10}$  shows intrinsic self-activated luminescence of a single broad band with a peak at 520 nm, extending from about 400 nm to 720 nm. Same emission band is obtained from micro- and nano-particles. It is suggested that the broadening of the emission band arises from single  $[\text{VO}_4]^{3-}$  molecule. This emission band is asymmetric, which is decomposed to two emission bands,  $\text{Em}_1$  and  $\text{Em}_2$ , due to the electronic transitions from the  ${}^3\text{T}_2$  and  ${}^3\text{T}_1$  excited states to  ${}^1\text{A}_1$  ground state in  $[\text{VO}_4]^{3-}$  centers, respectively. Same emission band is obtained from micro- and nano-particles. Each of the PLE spectra for the  $\text{Em}_1$  and  $\text{Em}_2$  emissions of  $\text{Cs}_5\text{V}_3\text{O}_{10}$  micro-particles consists of the same peaks at 280 and 365 nm which are called  $\text{Ex}_1$  and  $\text{Ex}_2$ , respectively. These  $\text{Ex}_1$  and  $\text{Ex}_2$  bands are attributed to the transitions from the ground state  ${}^1\text{A}_1$  to the  ${}^1\text{T}_2$  and

${}^1\text{T}_1$  states, respectively. The excitations into the  $\text{Ex}_1$  and  $\text{Ex}_2$  bands give the same emission band. In addition to the decay curve profiles of the  $\text{Em}_1$  and  $\text{Em}_2$  emission, the emission profiles indicate that the emission is due to not different kinds of  $[\text{VO}_4]^{3-}$  centers but only one kind of  $[\text{VO}_4]^{3-}$  center. When temperature is increased from 10 K to 450 K, the emission intensity increases below 150 K and decrease above 150 K, and unusual blue shift is observed. The emission lifetime becomes short largely above 150 K with increasing temperature. The observed temperature dependences are understood by the thermal feeding by the lower-energy  ${}^3\text{T}_1$  state to the higher-energy  ${}^3\text{T}_2$  state, which is effective above about 50 K, and by the thermal activation process from the  ${}^3\text{T}_2$  state to the  ${}^1\text{A}_1$  state which is effective above 150 K.

## Acknowledgements

This research was supported by Basic Science Research Program through the National Research Foundation of Korea (NRF) funded by the Ministry of Science, ICT & Future Planning (NRF-2013R1A1A2009154) and by the Priority Academic Program Development of Jiangsu Higher Education Institutions (PAPD), China.

## References

- 1 V. A. Ilchev, A. P. Pushkarev, R. V. Romyantsev, A. N. Yablonskiy, T. V. Balashova, G. K. Fukin, D. F. Grishin, B. A. Andreev and M. N. Bochkarev, *Phys. Chem. Chem. Phys.*, 2015, **17**, 11000-11005
- 2 N. F. Santos, J. Rodrigues, T. Holz, N. B. Sedrine, A. Sena, A. J. Neves, F. M. Costa and T. Monteiro, *Phys. Chem. Chem. Phys.*, 2015, **17**, 13512-13519.
- 3 C. Rohner, I. Tavernaro, L. Chen, P. J. Klar and S. Schlecht, *Phys. Chem. Chem. Phys.*, 2015, **17**, 5932-5941.
- 4 X. Wang, L. Zhang, J. Yang, F. Liu, F. Dai, R. Wang and D. Sun, *J. Mater. Chem. A*, 2015, **3**, 12777-12785.
- 5 J. Zhou, F. Huang, J. Xu, H. Chen and Y. Wang, *J. Mater. Chem. C*, 2015, **3**, 3023-3028
- 6 W. Su, T. Honda, T. Masui and N. Imanaka, *RSC Adv.*, 2013, **3**, 24941-24945
- 7 Wang, X. Liu, *Account Chem. Res.* 2014, **47**, 1378-1385.
- 8 X. Li, M. Yu, Z. Hou, G. Li, P. Ma, Z. Cheng, J. Lin, *J. Solid State Chem.*, 2011, **184**, 141-148.
- 9 J.H. Wu, B. Yan, *J. Alloys Compd.*, 2008, **455**, 485-488.
- 10 H. D. Nguyen, S. I. Mho, I. H. Yeo, *J. Lumin.*, 2009, **129**, 1754-1758.
- 11 P.J. Morris, W. Lulty, H.P. Weber, Y.D. Zavarstev, P.A. Studenikin, I. Shcherbakov, A.I. Zagumenyi, *Opt. Commun.*, 1994, **111**, 493-496.
- 12 T. Nguyen, M. Castaing, T. Gacoin, J. Boilot, F. Balembois, P. Georges, A. Alexandrou, *Opt. Express*, 2014, **22**, 20542-20550.
- 13 F. Wang, X.J. Xue, X.G. Liu, *Angew. Chem. Int. Ed.*, 2008, **47**, 906-909.
- 14 M. R. Dolgos, A. M. Paraskos, M. W. Stoltzfus, S. C. Yarnell and P. M. Woodward, *J. Solid State Chem.*, 2009, **182**, 1964-1971.
- 15 T. Nakajima, M. Isobe, T. Tsuchiya, Y. Ueda and T. Kumagai, *Nat. Mater.*, 2008, **7**, 735-740.
- 16 T. Nakajima, M. Isobe, T. Tsuchiya, Y. Ueda and T. Kumagai, *J. Lumin.*, 2009, **129**, 1598-1601.
- 17 H. Ronde and G. Blasse, *J. Solid State Chem.*, 1976, **17**, 339-341.
- 18 H. Ronde and G. Blasse, *J. Inorg. Nucl. Chem.*, 1978, **40**, 215-219.

- <sup>19</sup> A. A. Setlur, H. A. Comanzo, A. M. Srivatava and W. W. Beers, *J. Electrochem. Soc.*, 2005, **152**, 205-208.
- <sup>20</sup> T. Nakajima, M. Isobe, T. Tsuchiya, Y. Ueda, T. Manabe, *J. Phys. Chem. C*, 2010, **114**, 5160-5167.
- <sup>21</sup> H. Ronde and J. G. Snijder, *Chem. Phys. Lett.*, 1977, **50**, 282-283.
- <sup>22</sup> D. Song, C. Guo, T. Li, *Ceramics Inter.*, 2015, **41**, 6518-6524.
- <sup>23</sup> Y. F. Pu, Y. L. Huang, T. Tsuboi, W. Huang, C. L. Chen and H. J. Seo, *Mater. Lett.*, 2015, **149**, 89-91.
- <sup>24</sup> M. J. Bowers, J. R. McBride and S. J. Rosenthal, *J. Am. Chem. Soc.*, 2005, **127**, 15378-15379.
- <sup>25</sup> M. Wang, Y. Shi, G. Jiang, *Mater. Res. Bull.*, 2012, **47**, 18-23.
- <sup>26</sup> N.J. Turro, *Modern Molecular Photochemistry*, University Sci. Books (Sausalito, USA, 1991).
- <sup>27</sup> B. Liu, C. Shi, Q. Zhang, Y. Chen, *J. Alloys Compd.*, 2002, **333**, 215-218.
- <sup>28</sup> S. Tongay, J. Suh, C. Ataca, W. Fan, A. Luce, J. S. Kang, J. Liu, C. Ko, R. Raghunathanan, J. Zhou, F. Ogletree, J. Li, J. C. Grossman and J. Wu, *J. Sci. Rep.*, 2013, **3**, 2657-2661.
- <sup>29</sup> T. Schmidt, K. Lischka and W. Zulehner, *Phys. Rev. B*, 1992, **45**, 8989-8994.
- <sup>30</sup> E. R. Dohner, A. Jaffe, L. R. Bradshaw and H. I. Karunadasa, *J. Am. Chem. Soc.*, 2014, **136**, 13154-13157.
- <sup>31</sup> C. Netzel, V. Hoffmann, T. Wernicke, A. Knauer, M. Weyers, M. Kneissl and N. Szabo, *J. Appl. Phys.*, 2010, **107**, 033510-033518.
- <sup>32</sup> C. W. Struck and W. H. Fonger, *J. Lumin.*, 1970, **1**, 456-469.
- <sup>33</sup> W. H. Fonger and C. W. Struck, *J. Chem. Phys.*, 1970, **52**, 6364-6472.
- <sup>34</sup> C. W. Struck and W. H. Fonger, *J. Appl. Phys.*, 1971, **42**, 4515-4516.
- <sup>35</sup> S. Schwung, D. Enseling, V. Wesemann, D. Rytz, B. Heying, U. C. Rodewald, B. Gerke, O. Niehaus, R. Pöttgen and T. Jüstel, *J. Lumin.*, 2015, **159**, 251-257.
- <sup>36</sup> J. S. Kim, Y. H. Park, S. M. Kim, J. C. Choi and H. L. Park, *Solid State Commun.*, 2005, **133**, 445-448.
- <sup>37</sup> W.B. Fowler, *Physics of Color Centers*, Academic Press, New York, 1968.
- <sup>38</sup> H. Liu, Y. Zhang, L. Liao, Z. Xia, *J. Lumin.*, 2014, **156**, 49-54.